# Pyrolysis of Silica-Immobilized Benzyl Phenyl Ether: Competing Radical Rearrangement Pathways under Restricted Diffusion

A. C. Buchanan, III,* Phillip F. Britt, J. Todd Skeen, John A. Struss, and Chanda L. Elam

*Chemical & Analytical Sciences Division, Oak Ridge National Laboratory, P.O. Box 2008, MS-6197, Oak Ridge, Tennessee 37831-6197*

*Received August 17, 1998*

Pyrolysis studies of silica-immobilized benzyl phenyl ether (≈$PhOCH_2Ph$ or ≈BPE), a model for related ether structures in fuel resources, have been conducted at 275−325 °C to examine the impact of restricted mass transport on the pyrolysis mechanism compared with previous studies in fluid phases. Significant rearrangement chemistry is observed for ≈BPE occurring through two competitive free-radical pathways that are both promoted by the diffusional constraints. One path involves recombination of incipient benzyl and surface-bound phenoxy radicals to form benzylphenol isomers, **10**. The second, previously unreported rearrangement path for ≈BPE involves a 1,2-phenyl shift in an intermediate radical, ≈PhOCH·Ph, leading to formation of benzhydrol (**8**) and benzophenone (**9**) as principal products. The rearrangement products **8**−**10** typically account for ca. 50% of the pyrolysis products. However, the path selectivity is a sensitive function of ≈BPE surface coverage and the presence of spacer molecules that either facilitate or hinder hydrogen atom transfer steps on the surface.

## Introduction

Pyrolysis forms the basis for many current and envisioned technologically important processes for conversion of fossil and renewable energy resources into volatile fuels and chemicals.[1] Previously, fundamental studies of pyrolysis mechanisms of organic model compounds, which contain functional groups and structural elements that are representative of related assemblies present in fuel materials, focused on bond cleavage reactions that are essential to breaking down the macromolecular structure of organic fuel resources into volatile species.[2] Recently, there has been increasing awareness of the importance of retrogressive bond forming reactions that establish more refractory structures and result in lower energy efficiency and yields of volatile products.[3] Retrogressive reactions have been most often associated with oxygen-containing functional groups, such as cross-linking via decarboxylation of carboxylic acids[4] and the condensation of phenols.[5] Much less is known about retrogressive reactions for ether-containing model compounds. The pyrolysis of benzyl phenyl ether (BPE) has been extensively investigated as a model for labile ether bridges.[6−12] BPE pyrolysis is initiated by homolytic scission of the weak (ca. 52 kcal $mol^{-1}$)[13] C−O bond, which occurs at $T \geq 275$ °C to produce benzyl and phenoxy radicals that hydrogen abstract from BPE or from an added hydrogen donor to produce toluene and phenol as dominant products (eq 1). However, recombination of the incipient radicals through coupling at phenoxy ring carbons has also been detected, which forms benzylphenol isomers in about 10−15% yield (eq 2). Although no additional bonds are formed, this rearrangement pathway

$$PhCH_2OPh \rightarrow PhCH_2^{\bullet} + PhO^{\bullet} \xrightarrow{[H]} PhCH_3 + PhOH \quad (1)$$

$$PhCH_2^{\bullet} + PhO^{\bullet} \rightarrow o\text{-},p\text{-}HOPhCH_2Ph \quad (2)$$

constitutes a retrogressive reaction, since it produces a more refractory diphenylmethane linkage (ca. 88 kcal $mol^{-1}$ for the $C_{sp^2} - C_{sp^3}$ bond in $PhCH_2Ph$, itself, which is stable at 400 °C[2]). Since this radical recombination pathway may contain a contribution from a cage effect,

(1) (a) Gavalas, G. R. *Coal Pyrolysis*; Elsevier: Amsterdam, 1982. (b) Schlosberg, R. H. *Chemistry of Coal Conversion*; Plenum: New York, 1985. (c) Bridgwater, A. V., Ed. *Thermochemical Processing of Biomass*; Butterworth: London, 1984. (d) Stock, L. M. *Acc. Chem. Res.* **1989**, *22*, 427.

(2) Poutsma, M. L. *Energy Fuels* **1990**, *4*, 113.

(3) Malhotra, R.; McMillen, D. F. *Energy Fuels* **1993**, *7*, 227.

(4) (a) Eskay, T. P.; Britt, P. F.; Buchanan, A. C., III. *Energy Fuels* **1996**, *10*, 1257. (b) Eskay, T. P.; Britt, P. F.; Buchanan, A. C., III. *Energy Fuels* **1997**, *11*, 1278. (c) Manion, J. A.; McMillen, D. F.; Malhotra, R. *Energy Fuels* **1996**, *10*, 776.

(5) (a) Poutsma, M. L.; Dyer, C. W. *J. Org. Chem.* **1982**, *47*, 3367. (b) McMillen, D. F.; Chang, S.-J.; Nigenda, S. E.; Malhotra, R. *Prepr. Pap.−Am. Chem. Soc., Div. Fuel Chem.* **1985**, *30*, 414.

(6) (a) Meyer, D.; Nicole, D.; Delpuech, J. J. *Fuel Proc. Technol.* **1986**, *12*, 255. (b) Meyer, D.; Oviawe, P.; Nicole, D.; Lauer, J. C.; Clement, J. *Fuel* **1990**, *69*, 1309.

(7) (a) King, H.-H.; Stock, L. M. *Fuel* **1984**, *63*, 810. (b) King, H.-H.; Stock, L. M. *Fuel* **1982**, *61*, 1172.

(8) (a) Korobkov, V. Y.; Grigorieva, E. N.; Bykov, V. I.; Senko, O. V.; Kalechitz, I. V. *Fuel* **1988**, *67*, 657. (b) Korobkov, V. Y.; Grigorieva, E. N.; Bykov, V. I.; Kalechitz, I. V. *Fuel* **1988**, *67*, 663.

(9) (a) Schlosberg, R. H.; Davis, W. H., Jr.; Ashe, T. R. *Fuel* **1981**, *60*, 201. (b) Ozawa, S.; Sasaki, K.; Ogina, Y. *Fuel* **1986**, *65*, 707. (c) Wu, B. C.; Klein, M. T.; Sandler, S. I. *Energy Fuels* **1991**, *5*, 453. (d) Siskin, M.; Brons, G.; Vaughn, S. N.; Katrizky, A. R.; Balasubramamian, M. *Energy Fuels* **1990**, *4*, 488. (e) Suzuki, T.; Yamada, H.; Sears, P. L.; Watanabe, Y. *Energy Fuels* **1989**, *3*, 707. (f) Makabe, M.; Itoh, H.; Ouchi, K. *Fuel* **1990**, *69*, 575.

(10) Sato, Y.; Yamakawa, T. *Ind. Eng. Chem. Fundam.* **1985**, *24*, 12.

(11) (a) Yao, T.; Kamiya, Y. *Bull. Chem. Soc. Jpn.* **1979**, *52*, 492. (b) Kamiya, Y.; Yao, T.; Oikawa, S. In *Coal Liquefaction Fundamentals*; Whitehurst, D. D., Ed.; ACS Symposium Series 139; American Chemical Society: Washington, DC, 1980; pp 291−299.

(12) (a) Stein, S. E. *Am. Chem. Soc. Symp. Ser.* **1981**, *169*, 97. (b) Miller, R. E.; Stein, S. E. *Prepr. Pap.−Am. Chem. Soc., Div. Fuel Chem.* **1979**, *24*, 271.

(13) A C−O bond dissociation of 51.6 kcal $mol^{-1}$ is estimated from $\Delta H_f°(PhO^{\bullet}) = 9.6$,[14] $\Delta H_f°(PhCH_2^{\bullet}) = 48.5$,[14] and $\Delta H_f°(PhOCH_2Ph) = 6.5$ kcal $mol^{-1}$.[15]

10.1021/jo9816717 CCC: $15.00 
Published on Web 12/04/1998

which has been observed in supercritical solvents,[9c] it could be promoted in a diffusionally constrained macromolecular environment found in geo- and biopolymers.[16] Mass transport limitations are known to impact the kinetics, tar and char yields, and tar molecular weight distribution for coal pyrolysis.[1a,17] However, a molecular level understanding of the impact of mass transport limitations on pyrolysis reaction pathways is much more limited.[18]

We have been investigating the impact of restricted diffusion on pyrolysis reactions involving radical intermediates through the study of organic compounds covalently immobilized on a silica surface.[19] The chemistry and photochemistry of organic molecules in constrained media such as micelles, liquid crystals, organic crystals and polymers, layered clays, silica surfaces, and microporous zeolites is an active area of current chemical research.[20] Our use of the robust $Si-O-C_{aryl}$ tether for surface attachment to a nonporous silica nanoparticle (eq 3) permits an examination of the effects of diffusional

$$[SiO_2]Si-OH + ArOH \rightarrow [SiO_2]Si-O-Ar + H_2O \quad (3)$$

constraints over a wide range of chemical structure and temperature (up to ca. 450 °C).[18,19] Studies of silica-immobilized hydrocarbon models, in particular, α,ω-diphenylalkanes, have shown that restrictions on radical and molecular mobility can impact reaction rates and product selectivities even at high temperatures (typically 350−400 °C).[18,19] Restricted radical diffusion results in reduced rates of termination that can lead to the emergence or enhancement of radical chain pathways, particularly those involving unimolecular rearrangements and cyclizations. In this current study, we report the pyrolysis behavior of silica-immobilized benzyl phenyl ether (≈BPE, where ≈ represents the $Si-O-C_{aryl}$ linkage to the surface) at 275−325 °C. The diffusional constraints are found to produce a substantial enhancement in retrogressive chemistry (ca. 50% of the products) compared with corresponding fluid phase behavior, as a result of two competitive radical rearrangement pathways whose selectivity depends on surface coverage and the structure of neighboring molecules on the silica surface.

**Scheme 1**

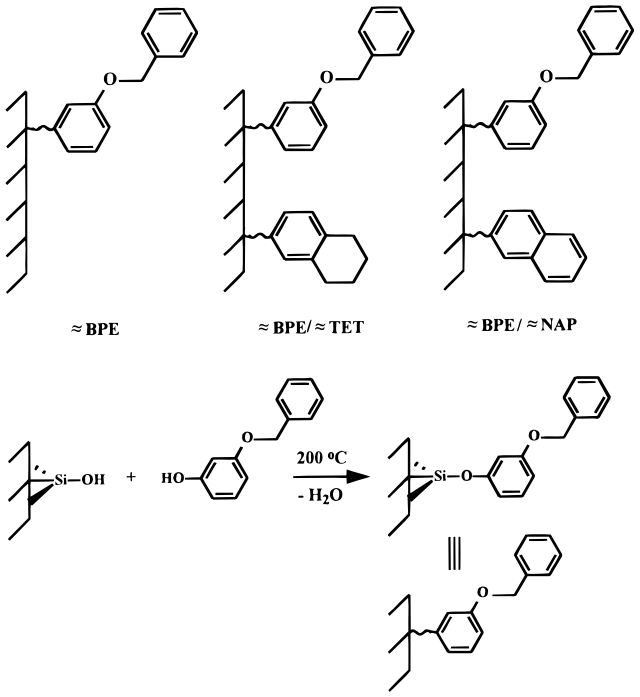


## Results and Discussion

**Preparation of Surface-Attached Substrates.** Silica-immobilized benzyl phenyl ether was prepared by the condensation of a phenolic precursor with the surface silanols of a high purity, amorphous, fumed silica (Scheme 1). This inert silica support is comprised of small nonporous particles (12 nm) with a surface area of 200 $m^2$ $g^{-1}$ and a fractal dimension of 2.08. Analysis of the silica surface before and after derivatization with phenols by FTIR and surface packing models has been previously described.[19a,b] Experience has shown that the remote silyloxy linkage to the surface results in only a minor substituent effect when in the *para* position that will be even further minimized with the currently employed *meta* linkage.[19b,c] Samples were prepared in which the ≈BPE surface coverage was varied from 0.084 to 0.24 mmol $g^{-1}$. Two-component surfaces were prepared by an analogous co-attachment procedure,[19a,e] which contained either an aromatic (naphthalene, or ≈NAP) or hydroaromatic (tetralin, or ≈TET) spacer molecule (Scheme 1). Reagent stoichiometries were adjusted to obtain ≈BPE surface coverages (ca. 0.07 mmol $g^{-1}$) that were comparable to the single-component ≈BPE surfaces at low surface coverages (0.084−0.094 mmol $g^{-1}$). This permits an evaluation of the effect of spacer molecular structure on the ≈BPE pyrolysis.

**Pyrolysis Products.** At least five pyrolyses were conducted on each sample at 275 °C in sealed, evacuated

(14) Britt, P. F.; Buchanan, A. C., III; Malcolm, E. A. *J. Org. Chem.* **1995**, *60*, 6523 and references therein.

(15) (a) Thermochemical estimate using group additivity.[15b,c] Corrections to reaction temperature were not applied since corrections involving $\Delta C°_p$ tend to be small and within the accuracy of the estimation procedures. (b) Benson, S. W. *Thermochemical Kinetics;* Wiley: New York, 1976. (c) Stein, S. E. NIST Structure and Properties Database, Version 2.0, 1994.

(16) (a) Green, T.; Kovac, J.; Brenner, D.; Larsen, J. W. In *Coal Structure*; Meyers, R. A., Ed.; Academic Press: New York, 1982; Chapter 6. (b) Berkowitz, N. *The Chemistry of Coal*; Elsevier: New York, 1985; Chapter 14. (c) Faulon, J.-L.; Hatcher, P. G. *Energy Fuels* **1994**, *8*, 402.

(17) (a) Solomon, P. R.; Fletcher, T. H.; Pugmire, R. J. *Fuel* **1993**, *72*, 587. (b) Serio, M. A.; Hamblen, D. G.; Markham, J. R.; Solomon, P. R. *Energy Fuels* **1987**, *1*, 138. (c) Suuberg, E. M. In *Chemistry of Coal Conversion*; Schlosberg, R. H., Ed.; Plenum Press: New York, 1985; Chapter 4. (d) Gilot, P.; Stanmore, B. R. *Energy Fuels* **1995**, *9*, 126.

(18) Buchanan, A. C., III; Britt, P. F. *J. Anal. Appl. Pyrolysis* In press.

(19) (a) Buchanan, A. C., III; Britt, P. F.; Thomas, K. B.; Biggs, C. A. *J. Am. Chem. Soc.* **1996**, *118*, 2182. (b) Buchanan, A. C., III; Dunstan, T. D. J.; Douglas, E. C.; Poutsma, M. L. *J. Am. Chem. Soc.* **1986**, *108*, 7703. (c) Buchanan, A. C., III; Biggs, C. A. *J. Org. Chem.* **1989**, *54*, 517. (d) Britt, P. F.; Buchanan, A. C., III. *J. Org. Chem.* **1991**, *56*, 6132. (e) Buchanan, A. C., III; Britt, P. F.; Thomas, K. B. *Energy Fuels* **1998**, *12*, 649. (f) Britt, P. F.; Buchanan, A. C., III; Malcolm, E. A.; Biggs, C. A. *J. Anal. Appl. Pyrolysis* **1993**, *25*, 407. (g) Buchanan, A. C., III; Britt, P. F. Biggs, C. A. *Energy Fuels* **1990**, *4*, 415.

(20) (a) Klafter, J.; Drake, J. M., Eds. *Molecular Dynamics in Restricted Geometries*; Wiley: New York, 1989. (b) Ramamurthy, V., Ed. *Photochemistry in Organized and Constrained Media*; VCH: New York, 1991. (c) Endo, K.; Koike, T.; Sawaki, T.; Hayashida, O.; Masuda, H.; Aoyama, Y. *J. Am. Chem. Soc.* **1997**, *119*, 4117. (d) Pitchumani, K.; Warrier, M.; Ramamurthy, V. *J. Am. Chem. Soc.* **1996**, *118*, 9428. (e) Turro, N. J.; Buchachenko, A. L.; Tarasov, V. F. *Acc. Chem. Res.* **1995**, *28*, 69. (f) Toda, F. *Acc. Chem. Res.* **1995**, *28*, 480. (g) Lem, G.; Kaprinidis, N. A.; Schuster, D. I.; Ghatlia, N. D.; Turro, N. J. *J. Am. Chem. Soc.* **1993**, *115*, 7009. (h) Laszlo, P. *Acc. Chem. Res.* **1986**, *19*, 121. (i) Leon, J. W.; Whitten, D. G. *J. Am. Chem. Soc.* **1995**, *117*, 2226.

**Scheme 2**

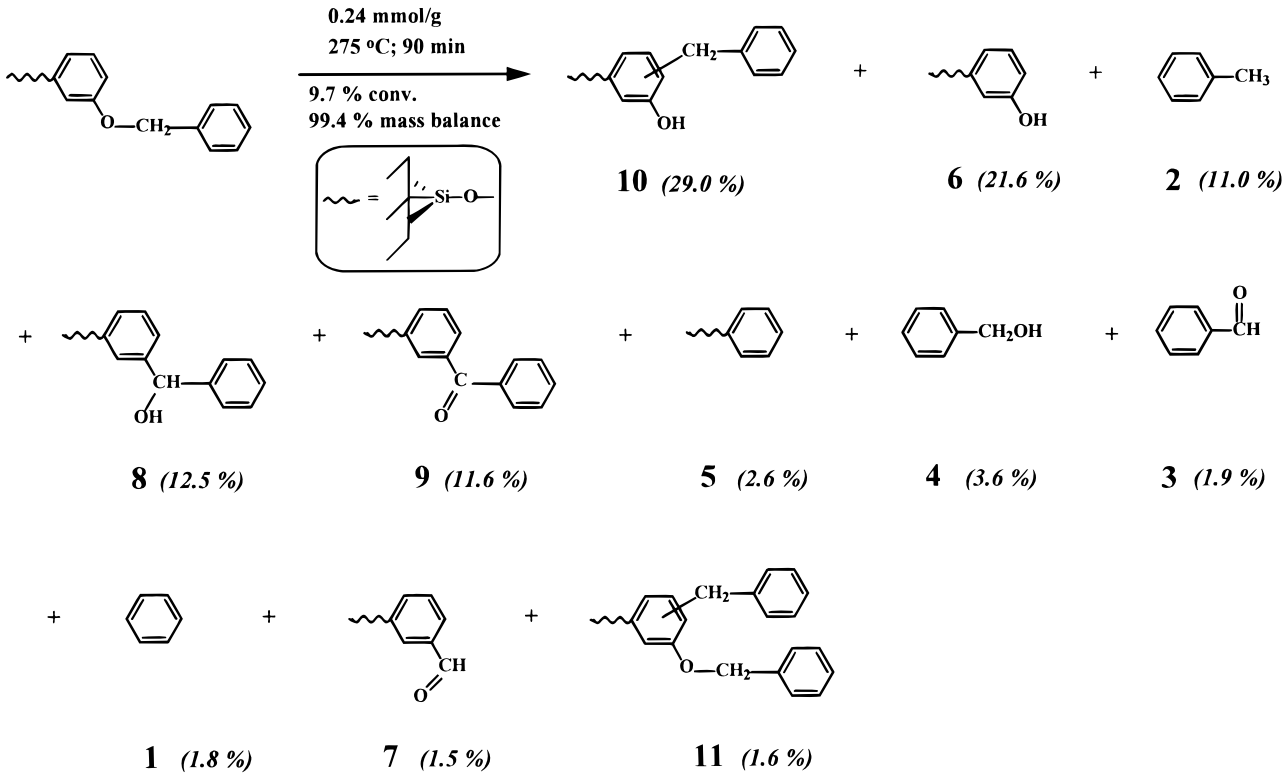


**Table 1. Principal Products from Pyrolysis of ≈$PhOCH_2Ph$ at 275 °C for 120 min**

| surface composition | ≈BPE | ≈BPE | ≈BPE | ≈BPE | ≈BPE/≈TET | ≈BPE/≈NAP |
|---|---|---|---|---|---|---|
| surface coverage (mmol/g) | 0.24 | 0.18 | 0.094 | 0.084 | 0.068/0.17 | 0.067/0.14 |
| ≈BPE charged (μmol) | 109 | 87 | 47 | 42 | 40 | 40 |
| total products (mol, rel)[a] | 16.8 | 14.8 | 20.5 | 22.6 | 13.4 | 9.2 |
| ≈BPE conversion[b] | 13.3 | 11.8 | 15.7 | 16.9 | 10.2 | 6.4 |
| mass balance (%)[c] | 102 | 97 | 97 | 95 | 96 | 96 |
| product distribution (mol %)[d] | | | | | | |
| PhH (**1**) | 1.7 | 2.0 | 2.0 | 2.6 | 1.7 | 0.9 |
| $PhCH_3$ (**2**) | 11.2 | 12.2 | 9.7 | 7.9 | 13.0 | 11.5 |
| PhCHO (**3**) | 1.6 | 1.9 | 1.6 | 1.4 | 0.8 | 1.7 |
| $PhCH_2OH$ (**4**) | 3.3 | 3.4 | 4.9 | 7.4 | 4.5 | 5.6 |
| ≈PhH (**5**) | 2.3 | 2.1 | 3.7 | 2.6 | 0.4 | 0.7 |
| ≈PhOH (**6**) | 21.7 | 21.5 | 22.9 | 26.4 | 20.3 | 32.8 |
| ≈PhCHO (**7**) | 1.4 | 1.6 | 1.3 | 1.4 | 0.3 | 1.0 |
| ≈PhCH(OH)Ph (**8**) | 12.5 | 10.5 | 6.9 | 6.2 | 8.2 | 3.9 |
| ≈PhC(O)Ph (**9**) | 12.4 | 11.4 | 8.8 | 6.7 | 13.9 | 5.5 |
| ≈$Ph(OH)CH_2Ph$ (**10**)[e] | 28.8 | 28.7 | 36.8 | 36.6 | 28.9 | 30.8 |
| ≈$Ph(CH_2Ph)OCH_2Ph$ (**11**)[e,f] | 1.6 | 2.2 | 0.7 | 0.4 | 0.3 | 0.3 |

[a] Molar sum of all products detected on a one hundred relative moles of ≈BPE basis. [b] Molar sum of all products detected calculated on a $C_{13}$ equivalents (≈BPE reacted) basis. [c] Sum of converted and unconverted ≈BPE. [d] Principal products whose structures are shown in Scheme 1. Products with a "≈" are attached to the silica surface and analyzed as the corresponding phenols following workup. [e] Multiple isomers, see text. [f] For ≈BPE/≈TET and ≈BPE/≈NAP, also detect analogous products involving benzyl addition to ≈TET (7.0 mol %) and ≈NAP (4.7 mol %).

tubes. An unexpectedly complex product mixture was obtained with the principal products shown in Scheme 2. Product distributions are compared for 120 min runs as a function of surface coverage and spacer molecule in Table 1. Volatile products (**1**−**4**) were collected in the cold trap and analyzed directly, while silica-attached products (**5**−**11**) were analyzed as the corresponding phenols following detachment from the surface by a base hydrolysis procedure. In pyrolyses of ≈BPE at 275 °C, excellent mass balances of 99 ± 2% were obtained over the conversion range studied (2.5−25.5%). The products shown in Scheme 2 typically accounted for > 98% of the products, with small amounts (<0.3%) of bibenzyl, stilbene, diphenylmethane, and several unidentified products also observed. For ≈BPE pyrolyses in the presence of either ≈TET or ≈NAP spacer molecules, the only new products detected in significant amounts (Table 1) resulted from benzyl radical addition to the spacer molecule (vide infra).

Typically, pyrolysis of BPE in fluid phases has been reported to yield phenol, toluene, and benzylphenols as the dominant products along with minor amounts of bibenzyl, diphenylmethane, and benzylated BPE (and benzylated aromatic solvent, if present). The distribution of pyrolysis products for silica-immobilized BPE is significantly altered compared with that in fluid phases. Particularly striking in Scheme 2 is the formation of major new products, alcohol **8** and ketone **9**, as well as the much enhanced yield of the immobilized benzylphenol **10** compared with the 10−15% yield typically found in

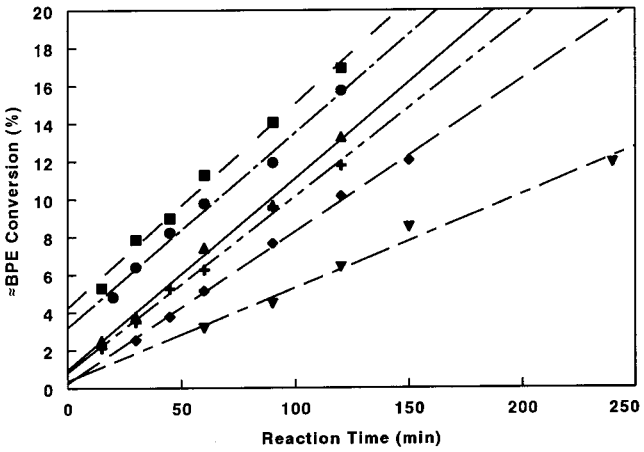


**Figure 1.** Initial rates for disappearance of ≈BPE at 275 °C: (■) ≈BPE (0.084 mmol $g^{-1}$), (●) ≈BPE (0.094 mmol $g^{-1}$), (+) ≈BPE (0.18 mmol $g^{-1}$), (▲) ≈BPE (0.24 mmol $g^{-1}$), (◆) ≈BPE/≈TET (0.068/0.17 mmol $g^{-1}$), (▼) ≈BPE/≈NAP (0.067/0.14 mmol $g^{-1}$).

**Table 2. Rate Data from Pyrolysis of ≈BPE at 275 °C**[a]

| surface composition | coverage (mmol $g^{-1}$) | rate × $10^4$ (% $s^{-1}$)[b] | corr coeff, $r$[c] | $k_{homol}$ × $10^5$ ($s^{-1}$)[d] |
|---|---|---|---|---|
| ≈BPE | 0.24 | 17 ± 0.6 | 0.998 | 1.5 ± 0.2 |
| | 0.18 | 16 ± 0.6 | 0.998 | 1.4 ± 0.2 |
| | 0.094 | 17 ± 0.8 | 0.995 | 3.0 ± 1.0[e] |
| | 0.084 | 18 ± 0.8 | 0.995 | 3.2 ± 1.0[e] |
| ≈BPE/≈TET | 0.068/0.17 | 14 ± 0.3 | 0.998 | 1.0 ± 0.1 |
| ≈BPE/≈NAP | 0.067/0.14 | 8.3 ± 0.6 | 0.988 | 0.74 ± 0.05 |

[a] Based on 5−6 pyrolyses for each sample. [b] Initial rates for total decomposition of ≈BPE determined from the slopes of linear regressions of ≈BPE conversion versus reaction time (see Figure 1) with reaction extent limited to <17%. [c] Correlation coefficient from linear regression analysis of initial rates. [d] Rate constants for homolysis of ≈BPE assuming first-order behavior. [e] Conversion dependent, see text.

fluid BPE pyrolysis. Although a discussion of mechanism and selectivity will be presented later, we note that the rearrangements that form **8**, **9**, and **10** establish the refractory diphenylmethane linkage and account for ca. 50% of the pyrolysis products. Since most of the fluid-phase pyrolyses of BPE have been conducted at 300−350 °C and higher BPE conversions, we conducted several pyrolyses on the 0.24 and 0.18 mmol $g^{-1}$ samples in this temperature range. At 300−325 °C, mass balances began to deteriorate to 87−91% at 45−50% conversion of ≈BPE. However, product distributions similar to those in Table 1 were obtained for ≈BPE conversions up to ca. 50%. Hence, the vastly different pyrolysis product distribution compared with that of the fluid phases is characteristic of the silica-immobilized BPE over a range of temperatures, ≈BPE surface coverages, and conversions. We will next discuss the kinetics of ≈BPE pyrolysis followed by an examination of the kinetics of the initial homolysis of the C−O bond.

**≈BPE Reaction Rates.** The rates for ≈BPE pyrolysis at 275 °C as a function of initial surface coverage and the presence of spacer molecules are shown in Figure 1. The initial rates for disappearance of ≈BPE reported in Table 2 were obtained from the slopes of the linear regression lines. For surfaces with ≈BPE alone, the initial rates obtained do not show any surface coverage dependence. However, for samples of ≈BPE, the regression lines in Figure 1 extrapolate to positive ≈BPE conversions at zero time, suggestive of a faster rate component for the very early stages of the reaction. It is also evident that this initial rate disturbance is magnified at the lower initial ≈BPE surface coverages.

Fumed silicas such as Cabosil contain an array of single and geminal silanols that exist in both isolated and hydrogen-bonded forms.[21] Since all silanol sites are not derivatized due to steric constraints,[19a,b] our hypothesis is that the fast rate component can be attributed to a small fraction of ≈BPE sites that are hydrogen bonded at the ether oxygen to underivatized silanols as illustrated below.

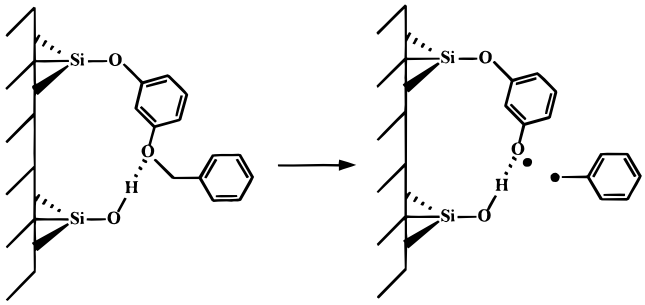


Consistent with this explanation are reports of acceleration of BPE pyrolysis in fluid phases upon addition of phenols[7b,11b] and tetrahydroquinoline[6b] as hydrogen-bonding agents. Furthermore, pyrolysis of anisole via scission of the O−$CH_3$ bond has been shown to be substantially accelerated by an *o*-hydroxy relative to a *p*-hydroxy substituent as a result of intramolecular hydrogen bonding available in the *o*-hydroxy case.[22] For ≈BPE pyrolysis, the enhancement of the initial fast rate component for the 0.084−0.094 mmol $g^{-1}$ samples is then a result of the presence of additional hydrogen-bonded sites at the lower surfaces coverages. If this explanation is correct, then the fast rate component observed at low ≈BPE surface coverages should be largely removed by derivatization of silanols with co-attached spacer molecules such as ≈TET and ≈NAP. As shown in Figure 1, this result was indeed realized. The spacer molecules also result in slightly lower values for the ≈BPE pyrolysis rate with the ≈NAP spacer having a larger effect. These decreases in ≈BPE pyrolysis rate are found to correlate to some degree with the rate constants for initial C−O homolysis, which are discussed below.

**Homolysis Kinetics.** In fluid phases, the initial homolysis of the weak C−O bond produces benzyl and phenoxy radicals (eq 1). Typically, homolysis rates have been measured in hydrogen donor solvents, such as tetralin, in an effort to capture most of the incipient radicals via hydrogen transfer and eliminate induced decomposition of the BPE. However, literature rate constants vary widely and range from 8 to 900 × $10^{-6}$ $s^{-1}$ at 300 °C.[6b,8,10,11a,12] This variation may, in part, be due to induced decomposition of BPE and catalysis by hydrogen bonding (vide supra) occurring to varying degrees. Studies by Sato and Yamakawa ($\log k/s^{-1} = (15.2-53.2)/2.303RT$)[10] and by Stein ($\log k/s^{-1} = (14.7-50.8)/2.303RT$)[12a] gave activation energies that are reasonably consistent with rate-controlling homolysis of the ca. 52 kcal $mol^{-1}$ C−O bond in BPE.[13]

(21) Liu, C. C.; Maciel, G. E. *J. Am. Chem. Soc.* **1996**, *118*, 5103.
(22) Hydrogen bonding resulted in a lowering of the O−$CH_3$ bond dissociation energy by 4.7 kcal $mol^{-1}$. Suryan, M. M.; Kafafi, S. A.; Stein, S. E. *J. Am. Chem. Soc.* **1989**, *111*, 1423.

**Scheme 3**

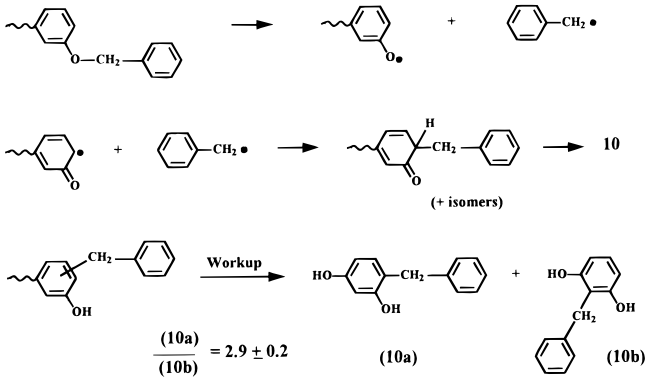


Pyrolysis of silica-immobilized BPE is also initiated by homolysis of the weak central C−O bond to produce gas-phase benzyl radicals and surface-immobilized phenoxy radicals (eq 4). As a result of induced decomposition reaction paths for ≈BPE, calculation of homolysis rate constants requires the fraction of ≈BPE reaction occurring through eq 4 to be identified. We chose to monitor the homolysis rate by following the fate of ≈PhO•, which undergoes only two reaction paths. The first is hydrogen abstraction, principally from ≈BPE at low conversions (eq 5), to form surface-attached phenol (toluene is formed analogously as shown in eq 6). The second path is recombination of ≈PhO• with $PhCH_2$• at

$$\approx PhO{-}CH_2Ph \rightarrow \approx PhO^{\bullet} + PhCH_2^{\bullet} \quad (4)$$

$$\approx PhO^{\bullet} + \approx PhOCH_2Ph \rightarrow \approx PhOH\ (\mathbf{6}) + \approx PhOCH^{\bullet}Ph \quad (5)$$

$$PhCH_2^{\bullet} + \approx PhOCH_2Ph \rightarrow PhCH_3\ (\mathbf{2}) + \approx PhOCH^{\bullet}Ph \quad (6)$$

phenoxy ring carbons to form benzylphenols **10** as shown in Scheme 3. Phenoxy radicals are well-known to undergo coupling reactions at ring carbon positions,[23] and silica gel is reported to catalyze the prototropic rearrangement of the keto intermediate to the enol tautomer.[23b] Although three isomers are possible from the radical recombination, two become equivalent following the base hydrolysis workup that generates **10a** and **10b** whose relative yields exhibit little variation with reaction conditions. Hence, the fate of phenoxy radicals can be described by the sum of **6** and **10**.

First-order rate constants for homolysis step 4 have been calculated at each time point at 275 °C (≈BPE conversions limited to <17%) using eq 7,

$$k_{homol} = (1/t)\ \ln\{(\approx BPE_0)/[(\approx BPE_0) - (x)]\} = (1/t)\ \ln\{100/(100 - x)\} \quad (7)$$

where $x$ is the extent of ≈BPE conversion to **6** + **10** in units of mol/100 mol of ≈BPE (Table 1) and $t = (t_{exptl} -$ 240 s) to account for the short heat-up period to reaction temperature. Calculated values and associated errors are reported in Table 2. For the high-coverage samples of 0.18 and 0.24 mmol $g^{-1}$, where there is minimal influence from the hydrogen bonding with surface silanols (vide supra),

(23) (a) Omura, K. *Tetrahedron* **1995**, *51*, 6901 and references therein. (b) Omura, K. *J. Org. Chem.* **1991**, *56*, 921.

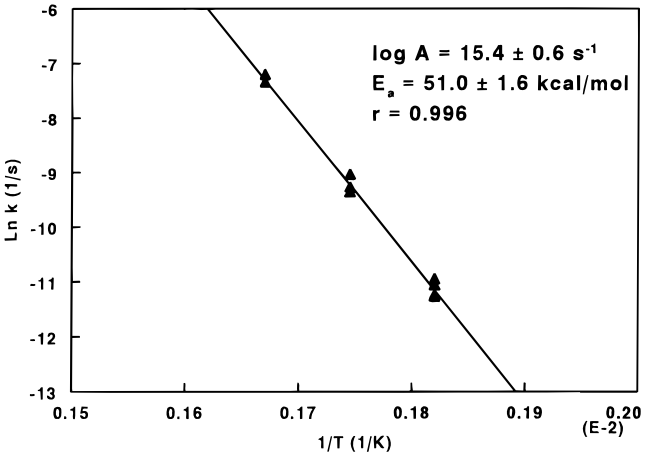


**Figure 2.** Temperature dependence of homolysis rate constant (10 values) for ≈BPE (0.24 mmol $g^{-1}$) at 275−325 °C.

the calculated rate constants were not sensitive to conversion and gave comparable values of ca. $1.5 \times 10^{-5}$ $s^{-1}$. Rate constants for the 0.24 mmol $g^{-1}$ sample were also measured at higher temperatures to permit determination of Arrhenius parameters that could be compared with the fluid-phase results. Arrhenius treatment of the ten pyrolyses at 275−325 °C (Figure 2) gave log $k/s^{-1} = (15.4 \pm 0.6) - (51.0 \pm 1.6)/2.303RT$. These Arrhenius parameters are in reasonable agreement with the values obtained in fluid phases[10,12a] and suggest that the silica surface causes little perturbation of the initial homolysis step at the highest surface coverages. However, for the samples of ≈BPE at lower surface coverages, the enhanced hydrogen bonding with surface silanols results in homolysis rate constants that are larger than those for the high-coverage samples (Table 2), which decrease in value with increasing reaction time as the concentration of hydrogen-bonded sites becomes depleted. For example, in the 0.094 mmol $g^{-1}$ sample, $k_{homol}$ ranges from 4.6 to $1.9 \times 10^{-5}$ $s^{-1}$ over the ≈BPE conversion range of 4.8−16%. These hydrogen-bonding effects are again suppressed by the presence of the co-attached ≈TET and ≈NAP spacer molecules resulting in rate constants that are not dependent on conversion and that have values of ca. $1 \times 10^{-5}$ $s^{-1}$.

**Pathways for Product Formation.** Following initial homolysis, radical recombination (Scheme 3) results in formation of **10** as discussed above. This product accounts for 29−37 mol % of the pyrolysis products over a range of surface coverages and spacer molecular structure (Table 1), whereas the corresponding product in fluid-phase BPE accounts for typically only 10−15 mol % of the pyrolysis products. Evidently, the restricted mass transport experienced by the surface-bound phenoxy radicals results in a substantially enhanced probability of radical recombination. The phenoxy and benzyl radicals that escape this recombination primarily undergo hydrogen abstraction from ≈BPE (eqs 5 and 6) to produce the major products **6** and **2**. The gas-phase benzyl radicals also undergo addition to ≈BPE to a small extent to produce **11**. In the presence of ≈NAP and ≈TET molecules, related products are detected from the parallel addition of benzyl radicals to these spacer molecules.

The formation of major new products, **8** and **9**, can be explained by rearrangement of the intermediate radical, ≈PhOCH•Ph, formed in hydrogen transfer steps 5 and 6, as shown in Scheme 4. This radical undergoes a 1,2-

**Scheme 4**

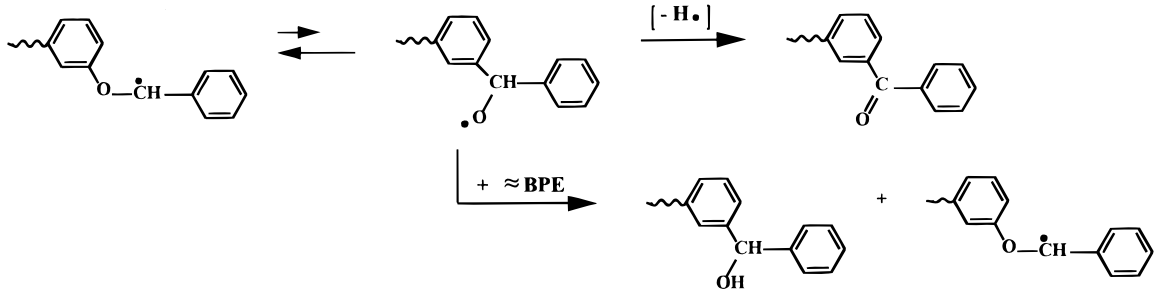


phenyl shift from oxygen to carbon followed by either hydrogen loss to form the benzophenone product **9** or hydrogen abstraction (principally from ≈BPE at low conversions) to form the benzhydrol product **8**. In Scheme 4, the hydrogen atoms produced in the formation of ketone **9** can react with ≈BPE by hydrogen abstraction to re-form ≈PhOCH•Ph. This rearrangement path that forms **8** and **9** then has the potential to develop radical chain character. The hydrogen atoms also competitively react with ≈BPE by standard *ipso*aromatic substitution to produce the minor hydrodealkylation products **1**, **3**, **4**, **5**, and **7**.[2] Hydrogen atoms are similarly generated from benzyl radical substitution onto the aromatic rings of ≈BPE and spacer molecules as described above.

The rearrangement path shown in Scheme 4 involves a highly reversible radical interconversion via an endothermic 1,2-phenyl shift followed by rate-limiting hydrogen transfer steps.[24] The proposed O−C phenyl shift has been detected previously in the pyrolysis of other aryl alkyl ethers, such as phenethyl phenyl ether[14] and phenetole.[26] Furthermore, in our previous studies of the pyrolysis of the structurally related silica-immobilized bibenzyl, we found that the diffusional constraints promoted an analogous rearrangement pathway involving a 1,2-phenyl shift in intermediate radical, ≈PhCH•$CH_2$-Ph, resulting in formation of silica-immobilized 1,1-diphenylethane in high yields.[19b,e] In studies of pyrolysis of fluid-phase BPE, this rearrangement path has not been reported, and related benzophenone and benzhydrol products have rarely been observed.[9e,f,10] It is possible that in experiments conducted under hydrogen-donating conditions, the small amounts of diphenylmethane product often reported arise from reduction of benzophenone and benzhydrol (if formed). However, the diffusional constraints imposed by surface immobilization clearly result in a significant enhancement in the rearrangement path for ≈BPE involving the 1,2 phenyl shift.

**Rearrangement Selectivity and Impact of Spacer Molecules.** Pyrolysis of surface-immobilized ≈BPE is dominated by two rearrangement pathways that are both enhanced compared with pyrolysis in fluid phases as a consequence of restrictions on diffusion for ≈BPE and the nascent ≈PhO•. For surfaces of ≈BPE alone, the radical recombination path that produces **10** (Scheme 3) and the rearrangement via phenyl shift (Scheme 4) that produces **8** and **9** account for ca. 50% of the pyrolysis products (Table 3). However, the results in Table 3 also show that the selectivity for the two rearrangement paths is a sensitive function of ≈BPE surface coverage and the structure of a co-attached spacer molecule. The selectivities were obtained from the ratio of the slopes of product yields versus time as illustrated in Figure 3. This approach was taken to determine the inherent path selectivities and to factor out the hydrogen-bonding effects that exaggerate the yields of **10** at short reaction times, particularly at low ≈BPE surface coverages (Figure 3). We note again that this perturbation is largely eliminated upon attachment of the spacer molecules.

**Table 3. Selectivity for Rearrangement Pathways in ≈BPE Pyrolysis**

| surface composition | coverage (mmol $g^{-1}$) | total rearr (mol %) **8** + **9** + **10**[a] | path select. **10**/(**8** + **9**)[b] |
|---|---|---|---|
| ≈BPE | 0.24 | 51.9 ± 1.3 | 1.00 |
| | 0.18 | 50.2 ± 1.8 | 1.34 |
| | 0.094 | 50.2 ± 1.5 | 1.78 |
| | 0.084 | 47.3 ± 1.6 | 2.04 |
| ≈BPE/≈TET | 0.068/0.17 | 54.3 ± 3.0 | 1.21 |
| ≈BPE/≈NAP | 0.067/0.14 | 40.7 ± 2.4 | 2.94 |

[a] Selectivity to rearrangement products based on 5−6 pyrolyses at 275 °C. [b] Path selectivity based on slopes of plots of product yields versus reaction time as shown in Figure 3.

For surfaces containing only ≈BPE, the path selectivity {**10**/(**8** + **9**)} is observed to increase as the ≈BPE surface coverage decreases. As the surface coverage decreases, molecules become increasingly separated on the silica surface. This results in decreased rates for bimolecular hydrogen transfer steps, particularly between two surface-bound species, as previously documented.[19] For example, the rate of hydrogen transfer step 5, which occurs between surface-bound phenoxy radicals and neighboring ≈BPE, should decrease with decreasing surface coverage. This step contributes to the generation of the key intermediate radical, ≈PhOCH•Ph, required for formation of **8** and **9**. Hence, at lower surface coverages, the selectivity for ≈BPE rearrangement via the radical recombination path becomes increasingly favored relative to the rearrangement path proceeding through ≈PhOCH•Ph.

Interestingly, the presence of the tetralin spacer, which can serve as a hydrogen donor to free radicals, is not effective at inhibiting the retrogressive rearrangement chemistry for ≈BPE. The rearrangement products still

(24) Thermochemical estimates[15] predict the overall rearrangement of $PhOCH_2Ph$ ($\Delta H_f° = 6.5$ kcal $mol^{-1}$) to PhCH(OH)Ph ($\Delta H_f° = -1.1$ kcal $mol^{-1}$) to have a favorable enthalpy change of $-7.6$ kcal $mol^{-1}$. However, the rearrangement of PhOCH•Ph ($\Delta H_f° = 33.3$ kcal $mol^{-1}$) to PhCH(Ph)O• ($\Delta H_f° = 50.8$ kcal $mol^{-1}$) by the 1,2-phenyl shift is estimated to be endothermic by ca. 17 kcal $mol^{-1}$ and, hence, will be highly reversible as found previously for the related rearrangement for the all-carbon analogue, $PhCH_2CH•Ph$.[19e] The heat of formation of PhOCH•Ph was estimated using group additivity[15b,c] with O−(C•)($C_B$) set equal to O−(C•)(C) = −23.0 kcal $mol^{-1}$ and C•-($C_B$)(H)(O) = C•−(C)(H)(O) + C•−($C_B$)$(H)_2$−C•−$(C)(H)_2$ = 18.7 kcal $mol^{-1}$. The heat of formation of PhCH(Ph)O• was estimated from PhCH(Ph)OH assuming an O−H bond dissociation energy of 104 kcal $mol^{-1}$, typical of other alcohols.[25]

(25) McMillen, D. F.; Golden, D. M. *Annu. Rev. Phys. Chem.* **1982**, *33*, 493.

(26) Collins, C. J.; Roark, W. H.; Raaen, V. F.; Benjamin, B. M. *J. Am. Chem. Soc.* **1979**, *101*, 1877.

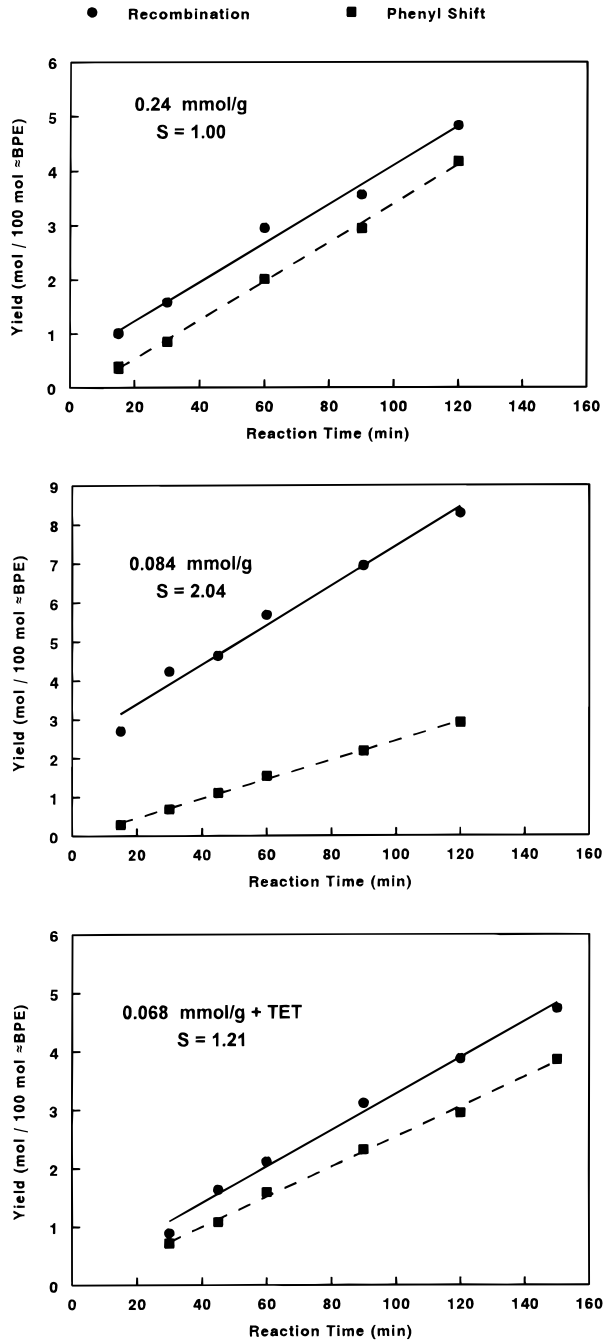


**Figure 3.** Product yields versus reaction time for rearrangement via (●) recombination path to form **10** (Scheme 3) and (■) phenyl shift path to form **8** + **9** (Scheme 4) for ≈BPE at high and low surface coverage and in the presence of ≈TET spacer. Path selectivity values, *S*, obtained from the ratio of slopes of the regression lines are reported for these and other samples in Table 3.

account for > 50% of the pyrolysis products. However, the rearrangement path selectivity is altered compared with that of similar low surface coverages of ≈BPE without spacer (Table 3). The enhanced selectivity for the recombination relative to the phenyl shift path observed for lower surface coverages of ≈BPE is largely removed by the presence of the neighboring tetralin molecules. A few pyrolyses were also conducted on a ≈BPE/≈TET sample (coverage of 0.022/0.30 mmol $g^{-1}$) with a much higher ≈TET/≈BPE mol ratio of 13.6. No significant differences were observed either in the amount of total rearranged products or in the path selectivity from the values reported in Table 3. The effect of the ≈TET spacer is readily understood in light of our recent discovery of a facile hydrogen transfer, radical relay mechanism that can occur for spacer molecules possessing benzylic C−H bonds.[19a] As illustrated in Scheme 5, this relay path alleviates some of the diffusional constraints experienced in hydrogen transfer steps that produce the key ≈PhOCH•Ph intermediate by reducing the separation between molecules and hydrogen-abstracting radicals on the surface. The relay process is facilitated by the preorganization of the molecules and radicals on the surface in a reduced dimensional reaction space.[19a]

In previous studies of pyrolysis of silica-immobilized bibenzyl in the presence of spacer molecules, we found that, as opposed to tetralin, naphthalene spacer molecules could act as barriers that retard the rate of hydrogen transfer steps on the surface. In the present case of ≈BPE, this would suggest that ≈NAP spacers should disfavor the rearrangement path involving phenyl shift and hydrogen transfer relative to the recombination path. As can be seen from Table 3, an enhanced selectivity favoring the recombination path was observed as expected. In addition to inhibition of the radical rearrangement path involving ≈PhOCH•Ph intermediates, the ≈NAP spacer also resulted in a decrease in the total amounts of rearranged products formed (Table 3), as well as a decrease in the ≈BPE pyrolysis rate.

## Conclusions

Pyrolysis studies of silica-immobilized benzyl phenyl ether have shown that restricted mass transport leads to a significantly altered product distribution compared with corresponding studies of BPE in fluid phases. Although the pyrolysis chemistry is still initiated by homolytic scission of the O−C bond to form phenoxy and benzyl radicals, the dominant products result from two rearrangement pathways. Radical recombination of the incipient radicals at phenolic ring carbons leads to the formation of surface-bound benzylphenols, whose yields are enhanced compared with fluid phases as a consequence of restricted diffusion for the immobilized phenoxy radicals. Furthermore, diffusional constraints result in the emergence of a previously unreported rearrangement pathway for BPE that forms significant amounts of surface-bound benzhydrol and benzophenone. This pathway, which involves a 1,2-phenyl shift in the ≈PhOCH•Ph radical followed by rate-limiting hydrogen transfer steps, appears to be of general significance under conditions of restricted diffusion. We have found related rearrangement pathways to be promoted in the pyrolysis of silica-immobilized bibenzyl and benzyl phenyl sulfide involving ≈$PhCH_2CH$•Ph[19b,e] and ≈PhSCH•Ph[27] intermediates, respectively.

The products from these two rearrangement pathways typically account for more than 50% of the products over a wide range of pyrolysis conditions. The formation of these products is not inhibited by the presence of neighboring hydrogen donor molecules on a surface such as tetralin. However, the selectivity for the two pathways is a sensitive function of the surface composition, with

(27) Ismail, K.; Mitchell, S. C.; Brown, S. D.; Snape, C. E.; Buchanan, A. C., III; Britt, P. F.; Franco, D. V.; Maes, I. I.; Yperman, J. *Energy Fuels* **1995**, *9*, 707. The kinetics of the related S−C phenyl shift in fluid phases have also been reported.[28]

**Scheme 5**

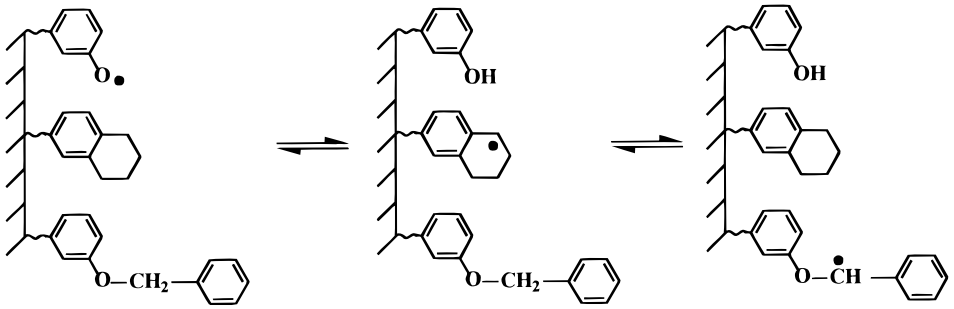


the radical recombination pathway favored by conditions that hinder hydrogen transfer steps on the surface (lower ≈BPE surface coverages and naphthalene spacers). Both rearrangement pathways can be considered retrogressive in nature, since the products **8**−**10** contain the more refractory diphenylmethane-type linkage rather than the labile ether bridge in ≈BPE. Furthermore, the products also contain reactive oxygen functional groups (ketone, alcohol, phenol) that can become involved in additional thermally induced, retrogressive reactions (formation of complex cyclic ethers, adduction to aromatics, reduction to diphenylmethanes, etc.).[5,29] This research suggests that related chemistry for aryl alkyl ethers in low-rank coals may contribute to the difficulty experienced in their thermochemical processing.

## Experimental Section

**General.** GC analysis was performed on a gas chromatograph employing a J & W Scientific 30 m × 0.25 mm DB-1 methylsilicone column (0.25 $\mu$m film thickness) and flame-ionization detection. Product detector response factors were determined relative to cumene (hydrocarbon products) or 3,4-dimethylphenol and *p*-phenylphenol (phenolic products) as internal standards. Mass spectra were obtained at 70 eV on a GC-MS equipped with a capillary column matched to that used for GC analyses. High-purity acetone, methylene chloride, and water were commercially available and used as received. Benzene was distilled from lithium aluminum hydride under argon before use. Commercially available cumene was fractionally distilled (2×), and 3,4-dimethylphenol and 4-phenylphenol were recrystallized (3×) from hexanes and benzene/hexanes, respectively, prior to use. The phenol *m*-$HOC_6H_4$-$OCH_2C_6H_5$ (HOBPE) was synthesized and purified (99.9% by GC) as previously described.[30] 2-Naphthol (HONAP) and 5,6,7,8-tetrahydro-2-naphthol (hydroxytetralin, or HOTET) were commercially available and were purified to >99.9% by reported procedures.[19e]

**Preparation of Surface-Attached Materials.** Preparation of surface-attached benzyl phenyl ether at various surface coverages followed the general methodology previously described for diphenylalkanes.[19] Cabosil M-5 silica (Cabot Corp., 200 $m^2\ g^{-1}$, ca. 4.5 SiOH $nm^{-2}$ or 1.5 mmol SiOH $g^{-1}$) was dried at 225 °C under vacuum for 4 h. HOBPE (2.715 g, 13.6 mmol) dissolved in dry benzene was added to a benzene slurry of silica (9.00 g, 13.5 mmol SiOH) and stirred for 0.5 h. Following solvent evaporation, the solid was sealed in an evacuated (2 × $10^{-6}$ Torr) Pyrex tube. The surface-attachment reaction was performed at 200 °C for 0.5−1.0 h in a fluidized sand bath. Unattached HOBPE was removed by Soxhlet extraction (6 h) with dry benzene under argon. The silica-attached BPE (≈BPE) was dried under vacuum, and surface coverage analysis (vide infra) gave a value of 0.24 mmol of BPE per gram of derivatized silica with a chemical purity of 98.3% by GC. Lower surface coverages of ≈BPE were prepared in a similar manner employing smaller HOBPE to silica ratios. HOBPE:SiOH ratios of 0.50, 0.12, and 0.11 resulted in ≈BPE surface coverages of 0.18, 0.094, and 0.084 mmol $g^{-1}$, respectively. Two-component surfaces were prepared by co-attachment in an analogous manner.[19a,e] The mol ratios of spacer phenol:HOBPE employed for HONAP:HOBPE and HOTET:HOBPE were 2.0 and 1.9, respectively, while the combined phenol:SiOH mol ratio was 1.0 for each sample. The resulting surface coverages for the silica-attached materials were 0.067/0.14 mmol $g^{-1}$ for ≈BPE/≈NAP and 0.068/0.17 mmol $g^{-1}$ for ≈BPE/≈TET. Surface coverage analysis was performed on 150−200 mg samples of surface-attached material dissolved in 30 mL of 1 N NaOH overnight. 4-Phenylphenol in 1 N NaOH was added as an internal standard. The solution was acidified with HCl (pH ≃4) and extracted with diethyl ether (3 × 10 mL). The combined ether layer was washed with 20 mL of brine, and the emulsion was separated by centrifugation. The ether phase was dried over $MgSO_4$ and filtered, and the solvent was removed under reduced pressure. Silylation with *N*,*O*-bis(trimethylsilyl)trifluoroacetamide (BSTFA) in pyridine (2.5 M, 0.30 mL) produced the corresponding trimethylsilyl ether. GC analysis of multiple assays provided surface coverages with a reproducibility of ±3%.

**Pyrolysis Procedure.** The pyrolysis apparatus and procedure have been described previously.[19] In brief, a weighed amount of sample (0.4−0.6 g) was placed in one end of a T-shaped Pyrex tube, evacuated, and sealed at ca. 2 × $10^{-6}$ Torr. The sample was inserted into a preheated temperature-controlled (±1.0 °C) tube furnace, and the other end was placed in a liquid nitrogen bath. The volatile products collected in the trap were dissolved in acetone (0.1−0.3 mL) containing internal standards (vide supra) and analyzed by GC and GC-MS. Surface-attached pyrolysis products were similarly analyzed after separation by digestion of the silica in aqueous base and silylation of the resulting phenols to the corresponding trimethylsilyl ethers as described above for the surface coverage analysis.

**Product Assignments.** Products **1**−**7** and **9** are commercially available and have been previously identified. Alcohol **8** was independently synthesized by the reduction of ketone **9** ($LiAlH_4$ in ether). Isomer **10b**, corresponding to 4-benzylresorcinol, was commercially available. Isomer **10a** is identified as 2-benzylresorcinol on the basis of similar unsilylated ($M_r$ = 200) and silylated ($M_r$ = 344) mass spectra compared with those of **10b** and on the basis of chemical reactivity considerations discussed in the text. Product **11**, formed from addition of benzyl radicals to ≈BPE, consisted of several overlapping isomers in the GC with $M_r$ = 290 that add one trimethylsilyl group upon silylation to give four isomers ($M_r$ = 362). Two of the principal isomers have mass spectra whose major fragmentation pathway involves loss of $PhCH_2$ ($m/z$ = 91) and suggests benzylation of the oxygen-substituted ring in ≈BPE as shown in Scheme 2. The other smaller isomers have as the dominant fragmentation pathway loss of

(28) Alnajjar, M. A.; Franz, J. A. *J. Am. Chem. Soc.* **1992**, *114*, 1052.
(29) Choi, C.-Y.; Stock, L. M. *J. Org. Chem.* **1984**, *49*, 2871.
(30) Buchanan, A. C., III; Britt, P. F.; Skeen, J. T. *Prepr. Pap.−Am. Chem. Soc., Div. Fuel Chem.* **1997**, *42*, 15.

$PhCH_2PhCH_2$ ($m/z = 181$) and suggest benzylation of the other phenyl ring. In the presence of the tetralin and naphthalene spacers, the only new pyrolysis products detected were from addition of benzyl radicals to the spacer molecules. In the tetralin case, four isomers ($M_r = 238$ unsilylated; $M_r = 310$ silylated) were detected, while in the naphthalene case, two isomers ($M_r = 234$ unsilylated; $M_r = 306$ silylated) were observed.

**Acknowledgment.** This research was sponsored by the Division of Chemical Sciences, Office of Basic Energy Sciences, U.S. Department of Energy, under contract DE-AC05-96OR22464 with Oak Ridge National Laboratory, managed by Lockheed Martin Energy Research, Corp.

JO9816717